

# We are IntechOpen, the world's leading publisher of Open Access books Built by scientists, for scientists

6,900

Open access books available

185,000

International authors and editors

200M

Downloads

Our authors are among the

154

Countries delivered to

TOP 1%

most cited scientists

12.2%

Contributors from top 500 universities



WEB OF SCIENCE™

Selection of our books indexed in the Book Citation Index  
in Web of Science™ Core Collection (BKCI)

Interested in publishing with us?  
Contact [book.department@intechopen.com](mailto:book.department@intechopen.com)

Numbers displayed above are based on latest data collected.  
For more information visit [www.intechopen.com](http://www.intechopen.com)



---

# Advances in Photoelectrochemical Fuel Cell Research

---

Kai Ren and Yong X. Gan

Additional information is available at the end of the chapter

<http://dx.doi.org/10.5772/50799>

---

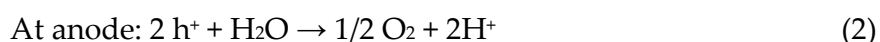
## 1. Introduction

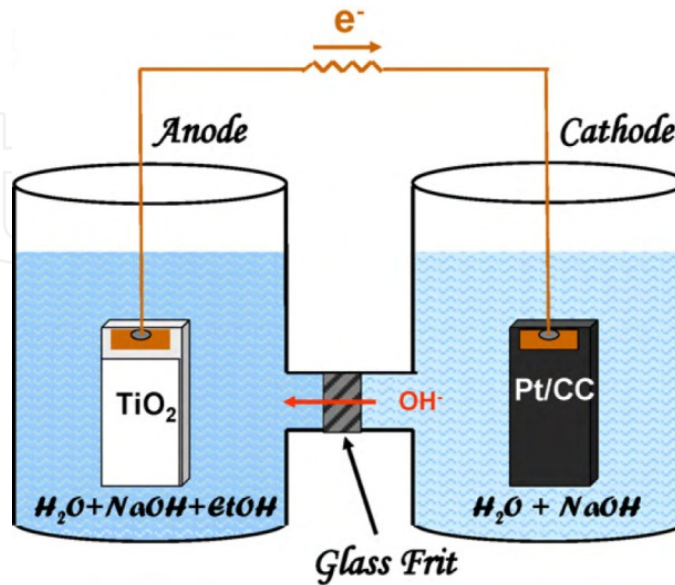
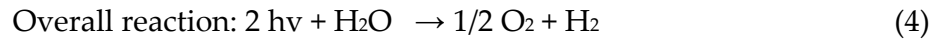
Fuel cells are electrochemical devices which can convert chemical energy into electrical power. They have the advantages of quiet in operation, high efficiency and low pollutant emissions. Photoelectrochemical fuel cells (PEFCs or PECs) are special fuel cells. PEFCs are used in organic waste degradation (Patsoura A et al., 2006), solar energy utilization (Bak T et al., 2002), gaseous product decomposition (Ollis DF et al., 2000), aqueous pollutants removal (Sakthivel S et al., 2004) and photocatalytic sterilization (Fujishima A et al., 1972). A PEFC or PFC consumes fuels and utilizes luminous energy to generate electricity power when the photoanode is excited by radiation. (Lianos P et al., 2010).

Fig. 1 shows a typical two-compartment photo fuel cell separated by a silica frit (Antoniadou M et al., 2010). The electrolyte is NaOH. The anode is nanocrystalline titania. The cathode is a carbon black deposited with Pt as the catalyst. This device works under UV irradiation. The open circuit voltage was 0.88V without ethanol and 1.22 V with ethanol.

## 2. Mechanisms of Photoelectrochemical Fuel Cells (PEFCs)

PEFCs normally consist of a semiconductor photoanode, metal cathode and electrolyte which could be an acid, base or just water. Light excites electrons at the photoanode if the light energy is larger than the material energy band gap. The photoanode generates electrons ( $e^-$ ) and holes ( $h^+$ ). At the anode, production of oxygen happens. Hydrogen generates at the water/cathode interface. The reactions are shown as follows (Chang C et al., 2012):

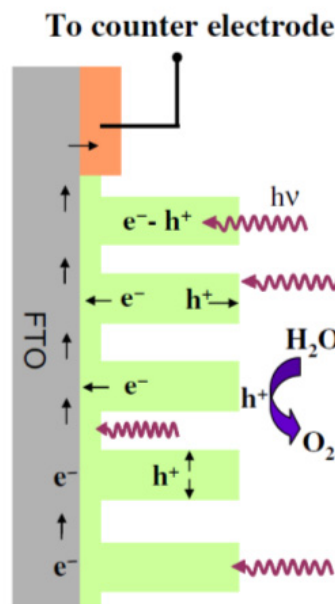




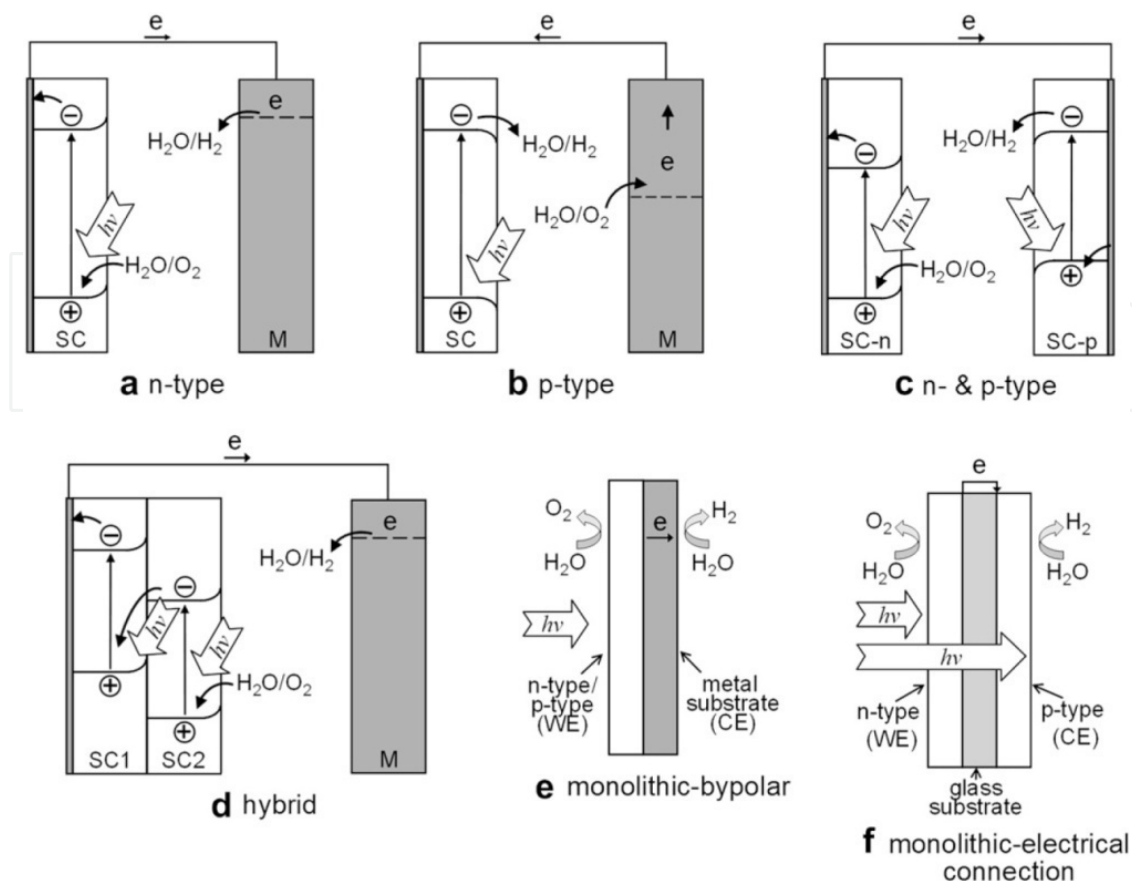
**Figure 1.** The sketch of a two-compartment PEFC. (Antoniadou M et al., 2010).

### 3. Photoanode materials

Fig. 2 shows light absorption and electron transport on a photo sensitive material. The light energy is absorbed by the photo sensitive material. Electrons and holes generate. The electrons flow to cathode. The holes decompose water to produce oxygen. Nanostructured materials may be added to substrates such as Ti, glass, copper etc.



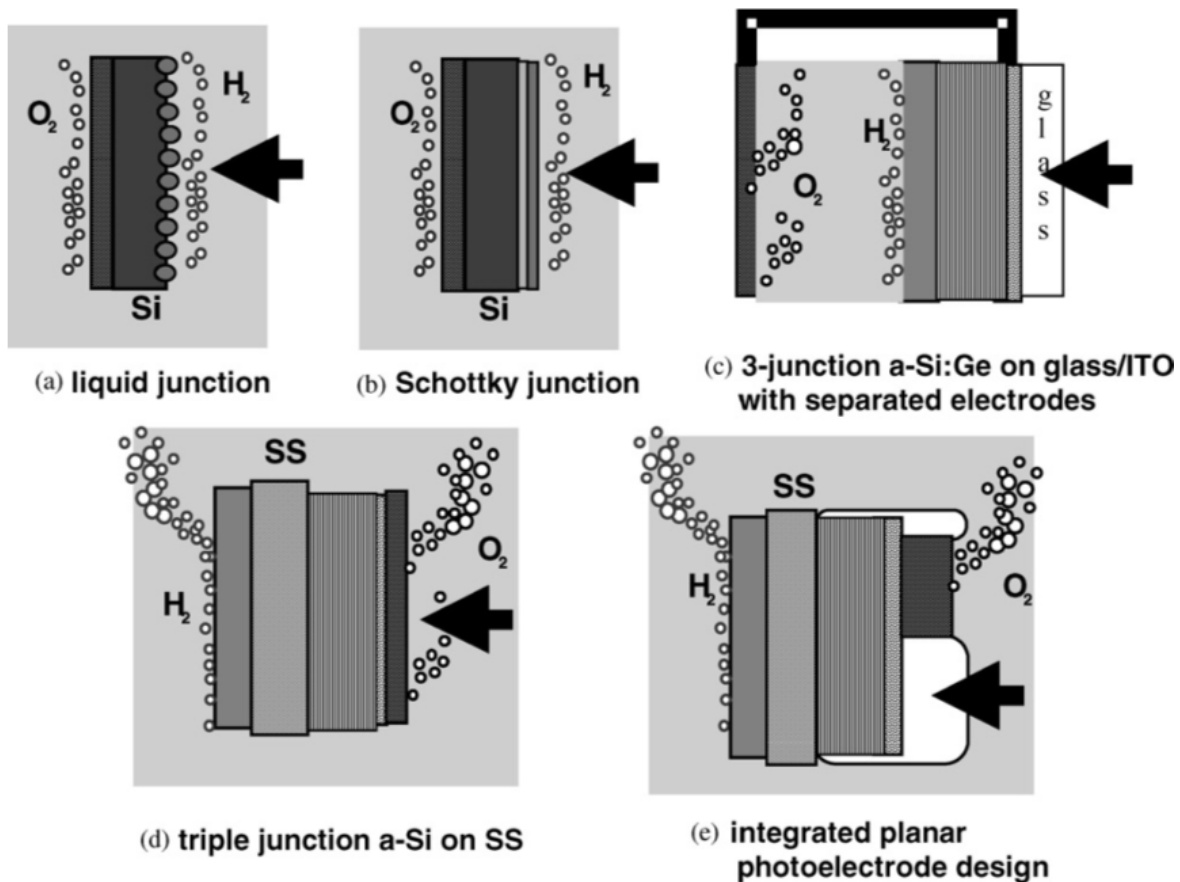
**Figure 2.** Schematic of a typical nanostructured photoanode. (Chakrapani V et al., 2009)



**Figure 3.** Some types of photoelectrode (PE) commonly used. (Minggu L et al., 2010).

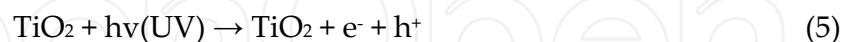
Semiconductor is widely used as photoelectrode which including n-type ( $\text{TiO}_2$ ), p-type (InP) and n-p type (n-GaAs/p-InP). They can be combined together to form multi-layered structures to tune the band gaps (Minggu L et al., 2010). In Fig. 3, SC stands for a semiconductor and M stands for a metal which is usually used as a substrate. Nanoporous materials are widely used in fuel cells. There are a number of transparent conductive oxides (TCOs) used as photoanode materials including indium-tin-oxide and fluorine-doped tin oxide. Some non-transparent conductive oxides (NTCOs) including nanocrystalline titania  $\text{TiO}_2$ , n-type semiconductor ZnO,  $\text{Fe}_2\text{O}_3$ ,  $\text{SrTiO}_3$  etc. can also be used as photoanode materials. Among them,  $\text{TiO}_2$  is the most commonly used one due to its stability and high photo activity.

Fig. 4 shows the design of photoelectrode (Miller EL et al., 2003). Fig. 4a shows the first stage of design using p-type silicon. The catalyst layer is on the left side and the platinum catalyst is deposited on the right side. The arrow indicates the direction of light illumination. In Fig. 4b, the right side is coated with a Schottky barrier metal. Fig. 4c illustrates a three-junction structure consisting of Si-Ge-glass. The photo-hydrogen conversion efficiency is up to 7.8%. This design needs an external connection. Fig. 4d has no external connection, as compared with Fig. 4c. Fig. 4e is the latest integrated planar photoelectrode design. On the right side, there is a highly transparent and corrosion-resistant film to keep the high efficiency. This new design can connect single cells in series, which can generate large power.



**Figure 4.** Photoelectrode designs. (Miller EL et al., 2003).

TiO<sub>2</sub> is an effective photocatalysis (PC). It is often used as the anode of PFC (Gratzel M et al., 2001). The reaction of TiO<sub>2</sub> under UV illumination is follows (Park KW et al., 2007):



This formula is applicable for any metal oxide as the anode in a photo fuel cell. When the metal oxide absorbs photons from any light sources, electron-hole pairs are produced. The photo-generated holes react with fuels.

#### 4. Fuels

There are many types of fuels for PECs including pure water, alcohols (MeOH, EtOH, PrOH), polyols (glycerol, xylitol, sorbitol, glucose, fructose, lactose), organic pollutants (urea, ammonia, triton X-100, SDS, CTAB). Alcohols have larger efficiencies than others do (Antoniadou M et al., 2009). In polyols, glycerol has the highest current density. Pure water has the lowest efficiency. Fuels are decomposed in the ways as described below.

Methanol (Lianos P, 2010):

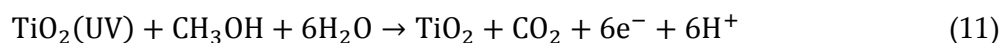
Anode electrode in acidic media :



Anode electrode in base media:

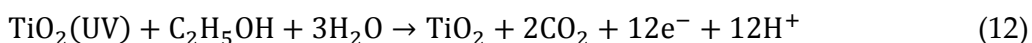


Under the photo illumination, PFC absorbs light energy and the  $\text{TiO}_2$  is excited to release electrons. By this method, higher electric potential can be generated compared with other fuel cells. The completely reaction of  $\text{TiO}_2$  with methanol's shown as:

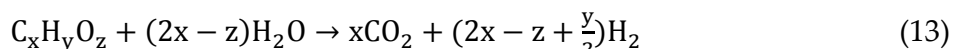


Ethanol:

The completely reaction of  $\text{TiO}_2$  with ethanol is as follows:



Reber JF et al., (1984) stated that a common formula could be:



Several types of biomass used in fuel cells are reported by Kaneko M et al., (2006), and shown in Table 1. The experimental condition is in acid solutions contain 0.1M  $\text{Na}_2\text{SO}_4$ . The anode of PEC is  $\text{TiO}_2$  nanoporous film and the cathode is Pt black on Pt foil. The light intensity is 503  $\text{mW}/\text{cm}^2$  and ambient temperature is 25 °C. The results of open circuit voltage show that acetic acid is the best. Ammonia, glycine, phenylalanine and glutamic acid also show good performances. The short circuit current of methanol has the highest value. The fill factor (FF) as defined by the ratio of maximum obtainable power to the product of the open circuit voltage and short circuit current was calculated. Ammonia has the maximum FF of 0.63.

Liu Y et al., (2011), did similar research on various fuels with a self-organized  $\text{TiO}_2$  nanotube array (STNA) as the photoanode of the photo fuel cell (Table 2). Multiply fuels were tested but each fuel's concentration was smaller than what Kaneko et al. used. By comparing the data in these two tables, we can see that the open circuit voltage and short circuit current obtained by Liu et al. are slightly larger, which means that they got higher efficiencies from the PFC system they built. When they varied the concentration of  $\text{Na}_2\text{SO}_4$  from 0 to 0.5M,  $V_{oc}$  and  $J_{sc}$  reached the peak values at 0.1 M and the FF has the maximum value at 0.05 M. All the experiments were done under solar light illumination.

Fuel (conc./M)	Solvent (pH)	V <sub>oc</sub> /V	J <sub>sc</sub> / mA cm <sup>-2</sup>	FF
Methanol	None	0.54	0.8	0.23
Methanol (50 vol.%)	Water (not controlled)	0.44	0.76	0.28
Ethanol	None	0.49	0.52	0.25
Glucose (0.5)	Water (5)	0.64	0.5	0.32
Urea (5)	Water (5)	0.6	0.3	0.26
Ammonia (10)	Water (12)	0.84	0.53	0.63
Acetic acid (2 wt.%)	Water (not controlled)	0.94	0.47	0.37
Glycine (0.5)	Water (5)	0.76	0.45	0.45
Glutamic acid (0.5)	Water (1)	0.9	0.64	0.42
Tyrosine (0.5)	Water (13)	0.86	0.43	0.36
Phenylalanine (0.5)	Water (13)	0.9	0.61	0.53
Agarose (0.2 wt.%)	Water (5)	0.6	0.12	0.26
Gelatin (2 wt.%)	Water (1)	0.64	0.23	0.32
Collagen (3 mg/ml)	Water (1)	0.62	0.16	0.34
Cellulose sulfate (2 wt.%)	Water (not controlled)	0.56	0.29	0.34
Lignosulfonic acid (0.5 wt.%)	Water (not controlled)	0.57	0.02	0.51
Polyethylene glycol (2 wt.%)	Water (5)	0.6	0.28	0.27
Poly(acrylamide) (2 wt.%)	Water (5)	0.6	0.23	0.24

**Table 1.** PFC performances by using different fuels in 0.1M Na<sub>2</sub>SO<sub>4</sub> with a TiO<sub>2</sub> photoanode and Pt/Pt black cathode. (Kaneko M et al., 2006).

	Organic compounds	V <sub>oc</sub> (V)	J <sub>sc</sub> (mA cm <sup>-2</sup> )	J <sub>vmax</sub> (mW cm <sup>-2</sup> )	FF
Model compound	Na <sub>2</sub> SO <sub>4</sub> (0.1 mol/L)	1.13	0.35	0.12	0.31
	Glucose (0.05 mol/L)	1.28	0.83	0.38	0.36
	Glutamic acid (0.05 mol/L)	1.34	1.08	0.51	0.35
	Nicotinic acid (0.05 mol/L)	1.39	0.61	0.3	0.35
	Acetic acid (0.05 mol/L)	1.48	1.42	0.67	0.32
	Urea (0.05 mol/L)	1.41	0.91	0.51	0.4
	Ammonia (0.05 mol/L)	1.24	0.72	0.37	0.41
	Actual wastewater	Pharmaceutical wastewater (COD =24572 mg/L)	0.88	1.36	0.43
Petroleum exploiting wastewater (COD =19087 mg/L)		1.34	0.98	0.34	0.26
Dying wastewater (COD =10842 mg/L)		1.53	1.21	0.5	0.27
Chemical plant wastewater (COD =11700 mg/L)		1.11	0.99	0.3	0.27
Original urine solution (COD =9642mg/L)		0.93	0.61	0.19	0.34

**Table 2.** PFC performances by using different fuels. (Liu Y et al., 2011).

## 5. Cathode materials

As compared with multiple choices of photoanodes, the materials for the cathode of photo fuel cells are limited. Normally a Pt wire or a Pt foil is used. Another option is to use Pt-black. The Pt black powders can be cast, sprayed or hot-pressed on the surface of a Pt (Kaneko M et al., 2006). The surface area becomes larger when the Pt-black powders were deposited onto Pt wires or foils. In addition to platinum cathodes including platinum wire, non-platinized platinum foil, platinized platinum foil, platinized SnO<sub>2</sub> with F, metal nanoparticles deposited on a TiO<sub>2</sub>/SnO<sub>2</sub> with F doping are made into electrodes. Pt/TiO<sub>2</sub>/SnO<sub>2</sub>, Pd/TiO<sub>2</sub>/SnO<sub>2</sub>, Au/TiO<sub>2</sub>/SnO<sub>2</sub>, Ag/TiO<sub>2</sub>/SnO<sub>2</sub>, and Ni/TiO<sub>2</sub>/SnO<sub>2</sub> are some of the examples. A platinum-loaded carbon cloth has also been used as a cathode material. The platinized SnO<sub>2</sub> with F electrode has better performance than others. Its current, voltage and efficiency are 1.15 mA/cm<sup>2</sup>, 1340 mV and 12.3%, respectively. The platinum-loaded carbon cloth has the maximum efficiency of 32.3%. Thin layer of Si-H film photo cathode can be made by plasma assisted chemical vapor deposition (PECVD). A Si-H cathode deposited organic or inorganic protective layer or coating with catalytic platinum can enhance the stability for long time use. The best thickness of the polymer protective layer is 5 nm. The optimized thickness of Pt coating is 2 nm.

CuO is a cheap material. CuO nanoparticles and films prepared by flame spray pyrolysis (FSP) were used as photocathodes by Chiang C et al., (2011). The optical band gap was decreased from 1.68 eV to 1.44 eV with the annealing temperature increasing from room temperature to 600°C. The nanoparticle size is from 50 nm to 150 nm, as shown in Fig. 5. The best photocurrent density is 1.2 mA/cm<sup>2</sup> obtained from CuO particles which were annealed at 600 °C for 3 hour. The bias voltage is 0.55 V in 1M KOH. The total conversion efficiency is 1.48% and the hydrogen generation efficiency is 0.91%.

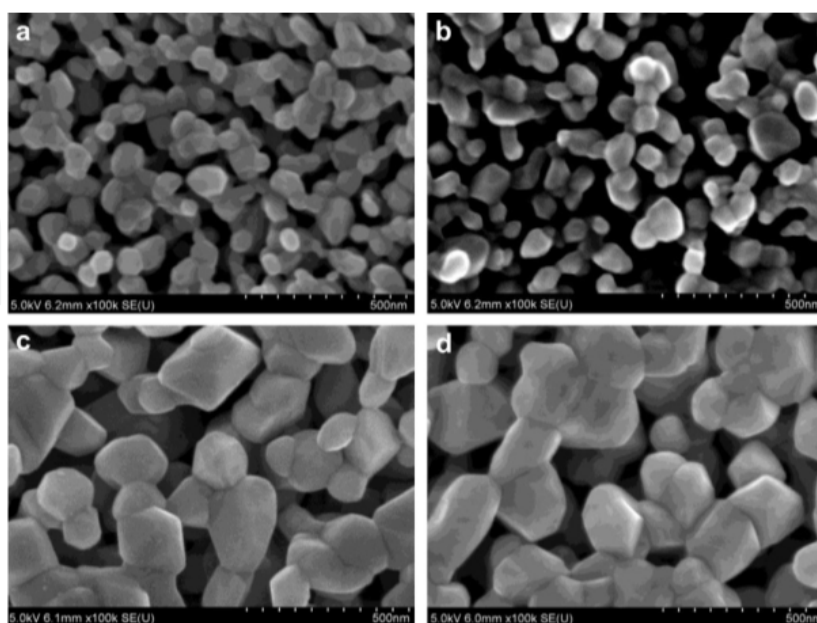


**Figure 5.** SEM images of CuO photo cathodes prepared under different conditions: (a) 450 °C, 1 h, (b) 450 °C, 3 h, (c) 600 °C, 1 h, (d) 600 °C, 3 h. (Chang C et al., 2011).

## 6. Terminologies associated with the photo fuel cells

### 6.1. Optical absorption coefficient for band gap determination

The optical absorption coefficient,  $\alpha$ , is related to the wavelength, transmittance, reflectance of the light illuminating on a material. Low absorption coefficient means low photo absorption ability. The following equation holds (Pihosh Y et al., 2009)

$$\alpha(h\nu) = d^{-1} \ln\left(\frac{1-R}{T}\right) \quad (14)$$

where T is the transmittance, R the reflectance, and d the thickness of the material. The term  $h\nu$  refers to the photon energy.

The optical coefficient is used to obtain the band gap  $E_g$  following

$$\text{constant} \times (h\nu - E_g)^2 = \alpha(h\nu) \times (h\nu) \quad (15)$$

### 6.2. Roughness factor

Roughness factor is related to the surface area of an electrode. For nanotubes, the geometry roughness is calculated as (Shankar K et al., 2007)

$$G = \left[ \frac{4\pi L(D+W)}{\sqrt{3(D+2W)^2}} \right] \quad (16)$$

where D is the inner diameter, W the wall thickness and L the tube length of the nanotubes. From the experiment on titania nanotubes by Isimjan TT et al., (2012), a higher surface area (roughness) was obtained at higher processing voltages. At a constant voltage, the pore size of nanotubes is dependent of distance between anode and cathode in the electrochemical process.

### 6.3. Photo conversion efficiency

The photo conversion efficiency is the overall efficiency of a PEC which can be defined by the following equation

$$\eta(\%) = \left[ \frac{(\text{total power output} - \text{electrical power output})}{\text{light power input}} \right] \times 100 \quad (17)$$

## 7. Nanostructures photoanode materials processing

### 7.1. TiO<sub>2</sub> nanotube (TNT) photoanode

TiO<sub>2</sub> nanotubes on the surface of Ti as shown in Fig. 6 demonstrate a self-organized nanostructure. The advantage of the nanobutes is the high surface/volume ratio. TiO<sub>2</sub> nanotubes have active photo catalysis characteristic, good corrosion resistance, thermal stability and good operation stability as described by Mahajan V et al., (2008). TiO<sub>2</sub> nanotubes can be made by various ways including hydro/solvothermal method (Kasuga T et

al., 1998), template-assisted approach (carbon nanotube, alumina or monocrystal as the template), sol-gel method (Kasuga T et al., 1998), microwave irradiation (Zhao Q et al., 2009), and direct electrochemical anodization. The advantage of the hydro/solvothermal method is easy to operate. The disadvantage is that only disordered and twisted  $\text{TiO}_2$  nanotubes can be obtained. For the template-assisted method, the size of the nanotubes is uniform. For the electrochemical anodic oxidation method, it has the advantage of easy to operate and the obtained nanotubes are highly ordered. Therefore, many researchers prefer the electrochemical method.

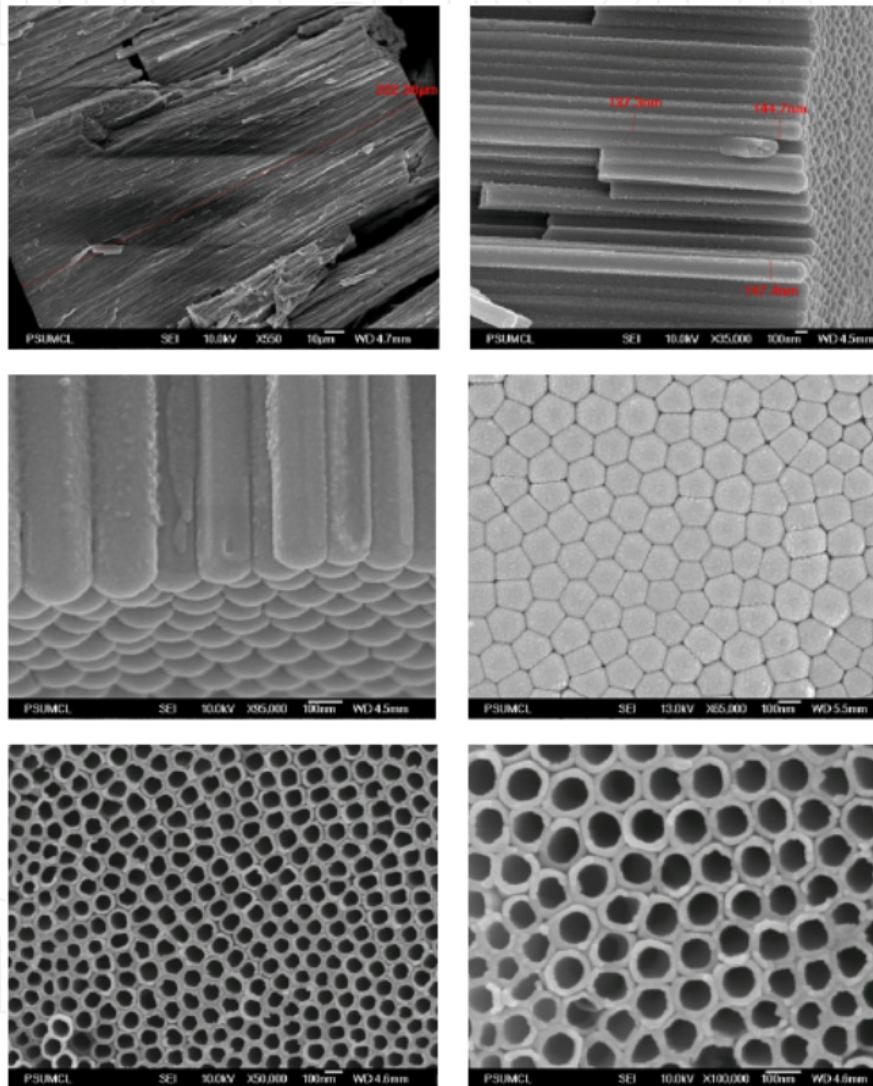


**Figure 6.** Self-organized  $\text{TiO}_2$  nanotubes via anodization. (Shankar K et al., 2007).

### 7.1.1. Hydrothermal treatment

Hydrothermal method is one of the popular approaches to prepare TNTs. The first group having successfully fabricated  $\text{TiO}_2$  nanotubes by hydrothermal method is Kasuga T et al., in 1998. During the process, titania nanopowders are placed in alkaline aqueous solutions held in high pressure steel vessels. The temperature should be between 50-180 °C. The process

continues for 10 to 20 hours. Some post treatment can be applied, for example, washing with acid or alkaline solutions for 10 hours, drying at 80 °C and annealing at 500 °C. The reaction process is divided into four steps (Hafez H et al., 2009) i.e. (1) synthesis of TiO<sub>2</sub> nanotubes in alkaline aqueous solutions, (2) protons replacing alkali ions in the reaction, (3) drying, (4) acid washing (post treatment). There is controversy about the necessity of the acid washing. Some researchers (Liu S et al., 2009) think acid washing is a necessary procedure to form TNTs, but other researchers (Chen X et al., 2007) think hydrothermal is more important than the acid washing step as sketched in Fig. 7. The step of washing by acid is not even necessary to form TNTs.

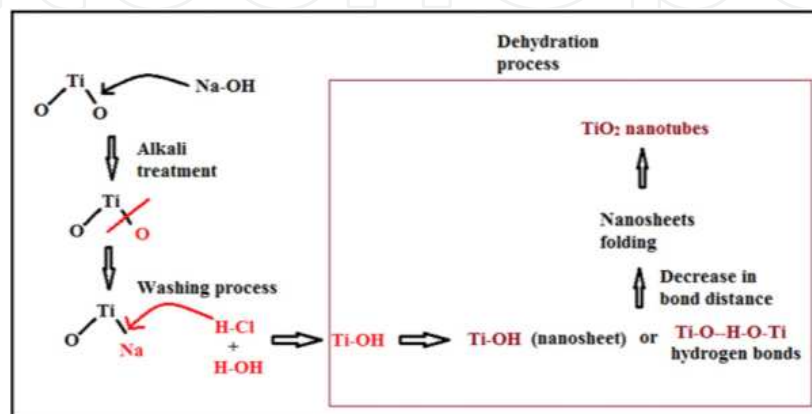


**Figure 7.** Hydrothermal method for fabricating TiO<sub>2</sub> nanotubes (Chen XB et al., 2007).

### 7.1.2. The effects factors of material and solution

With different raw materials and reaction solutions, the different morphology of TiO<sub>2</sub> was obtained by hydrothermal method (Yuan ZY et al., 2004). When crystalline TiO<sub>2</sub> react with NaOH under 100-160 °C, the TiO<sub>2</sub> nanotubes was obtained. When amorphous TiO<sub>2</sub> be used under same conditions, the TiO<sub>2</sub> nanofibers are fabricated. Either crystalline or amorphous TiO<sub>2</sub> can be used reaction with NaOH can result TiO<sub>2</sub> nanoribbons when temperature rise to 180 °C. If the solution used by KOH, the nanowires morphology is formed. The pH value of solution also plays an important role in morphology of TiO<sub>2</sub> nanomaterials (Xu YM et al., 2010). Fen LB et al., (2011) used anatase TiO<sub>2</sub> nanopowders (Aldrich 637254-50G, 99.7%) with NaOH solution fabricated TNTs. The inner diameter is 3-6 nm and wall thickness is 1.9 nm. Lan Y et al., (2005) used rutile nanopowders with 10 M NaOH solution obtained TNTs which inner diameter 2-3 nm and wall thickness is 7-8 nm, besides the length is 200-300 nm. The inner diameter is smaller but the wall thickness is larger than the TNTs made by Fen LB et al., (2011).

Hydrothermal treatment temperature and time are significant factors during the formation of TNTs. The temperature range should be from 100 °C to 180 °C and the time range should be from 1 to 24 hours. Sreekantan S et al., (2010), selected the temperatures at 90, 110, 130, 150 °C and time for 3, 6, 9, 15, 18, 24 hours. The NaOH/TiO<sub>2</sub> solution was used. At 90 °C, the TiO<sub>2</sub> particles form sheets. When the temperature was set at 110 °C, the sheets were transformed into nanotubes because the thermal energy increases with temperature (Seo HK

et al., 2008). With the temperature increasing to 130, 150 °C, there is no change of the outer diameter (10 nm) of nanotubes but the TNTs transform to anatase phase. For the effect of reaction time, particles begin to form sheet at 3 hours. Sreekantan S et al., (2010) indicated that Ti-O-Ti bond is replaced by Ti-O-Na and Ti-OH bonds at this time. After 6 and 9 hours, more and more sheets form nanotubes (10 nm). After 15 hours, TNTs form completely. They found that 150 °C is the best temperature for making TNTs with the highest photocatalytic activity.

Seo HK et al., (2008), studied the phase transformation of TNTs at different hydrothermal temperatures. They used a 10 M NaOH solution and the temperature range was from 70 °C to 150 °C. A 0.1 M HCl solution was used for washing the TNTs. They founded that at 70 °C, the particles begun forming nanosheets. Nanosheets and nanofibers co-existed at 90 °C. At 110 °C, the nanosheets were transformed into nanotubes. This conclusion is also reported by Sreekantan S et al., (2009). Hydrothermal processing can also produce nanoribbons instead of nanotubes if the reaction temperature is higher than 180 °C.

## 7.2. Synthesis of self-organized TiO<sub>2</sub> nanotubes via electrochemical anodization

In 1999, Zwillig V et al. first used electrochemical anodization method for synthesis of TiO<sub>2</sub> nanotubes in the solution containing chromic acid and hydrofluoric acid. Later many researchers (e.g. Macak JM et al., 2005) showed that using different applied potentials, electrolytes, pH values (much longer nanotubes at neutral pH electrolytes) and anodization time can control the lengths, thickness, diameters and morphology of TiO<sub>2</sub> nanotubes. Zeng X et al., (2011), reported electrochemical oxidation of Ti in a 1.0 M H<sub>3</sub>PO<sub>4</sub> and 0.25 M NaF solution. With the increasing in the potential, TiO<sub>2</sub> experienced three forms. When the potential was very low, Ti dissolved into the solution. With the increasing of potential, Ti was oxidized to form TiO<sub>2</sub>. When the potential was less than 2.5 V, TiO<sub>2</sub> film was obtained. Between 2.5 V and 6.0 V, the TiO<sub>2</sub> porous structure formed. When potential was higher than 6, the self-organized TiO<sub>2</sub> nanotubes were obtained (Fig. 9b).

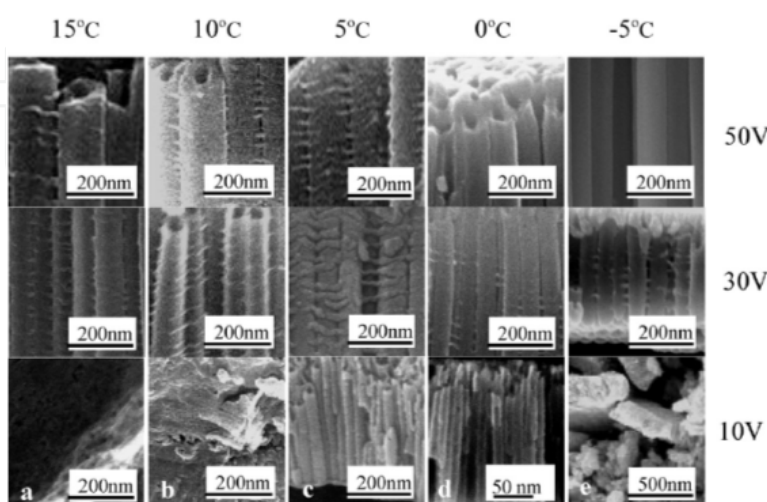


**Figure 8.** Morphology of self-organized anodic TiO<sub>2</sub> nanotubes formed at different temperature and voltage levels. (Liu H et al., 2011).

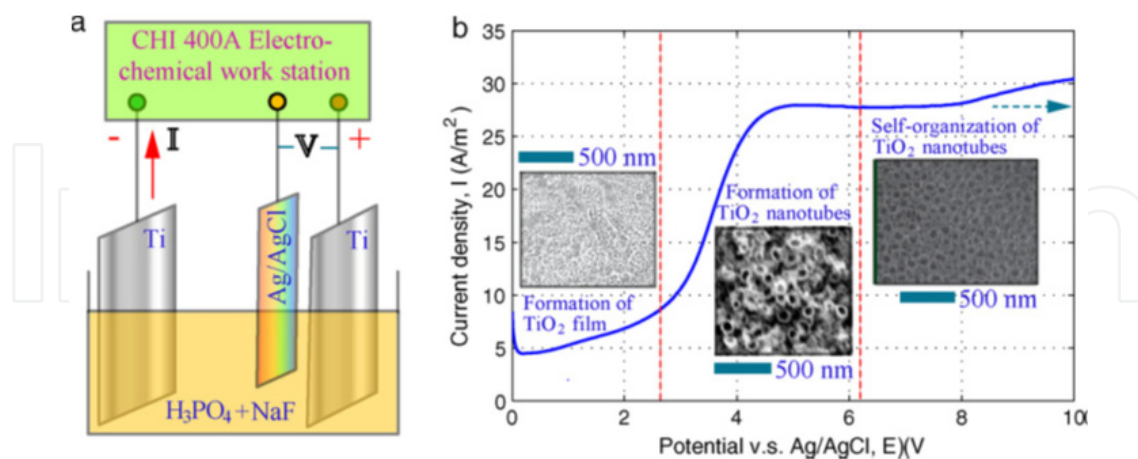


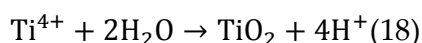
**Figure 9.** (a) Sketches for electrochemical oxidation of Ti. (b) effect of voltage level on the morphology of TiO<sub>2</sub>. (Zeng X et al., 2011).

Before 2005, all of these researches were exclusively using inorganic solutions as electrolytes, such as HF (Varghese OK et al., 2003), KF, NaF (Cai QY et al., 2005). Macak JM et al., (2005), investigated TiO<sub>2</sub> nanotube formation in Na<sub>2</sub>SO<sub>4</sub> electrolytes with NaF. The maximum length of nanotubes was up to 2.4 μm. It takes about 6 hours. But longer than this time, the irregular morphology showed up. As compared with HF, NaF can thicken the porous layers. The use of organic electrolytes is a milestone for the TiO<sub>2</sub> nanotubes fabrication. Liu H et al., (2011), studied the temperature effect on morphology of TiO<sub>2</sub> nanotubes. The specified temperatures are -5, 0, 5, 10, 15 °C and the applied potentials are 10, 30, 50V. It helped control the nanotube size and structure under the complex condition as show in Fig. 8. In summary, there are two types of electrolytes in TiO<sub>2</sub> anodization, one is aqueous-based electrolytes, and the other is organics-based electrolytes. Aqueous electrolytes allow the nanotubes to form more quickly because of the low electrical resistance. Besides, lower voltage is enough. However, it is hard to form longer nanotubes because of the dissolution of the nanotubes in the solutions. The organic electrolytes, for example, ethylene glycol and glycerol, have higher electrical resistances. They can slow down the ion transfer. Therefore, higher voltages and longer times are needed. In organic electrolytes, it is easier to form long nanotubes.

### 7.2.1. Anodization mechanisms

During anodization, a constant voltage in the range from 1V to 150V is applied. The electrolytes containing fluorides have the concentration range from 0.05 to 0.5M. The processing time ranges from a few minutes to a couple of days.

There are two main reactions with the anodization of Ti (Macak JM et al., 2005):



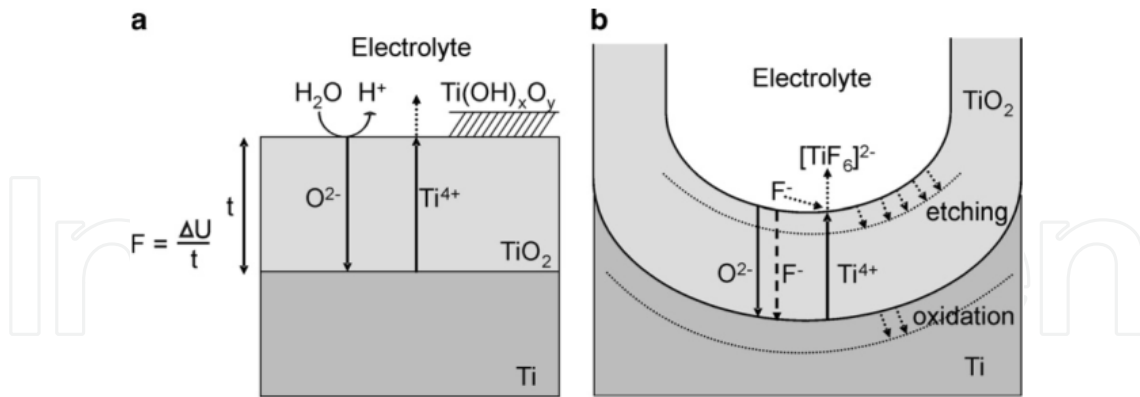
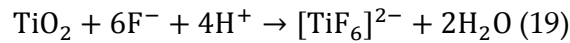


**Figure 10.** Sketches of Ti anodization (a) without  $\text{F}^-$ , (b) with  $\text{F}^-$ . (Macak JM et al., 2007).

First, titanium in the electrolyte produces  $\text{Ti}^{4+}$ . Then  $\text{Ti}^{4+}$  reacts with water to form  $\text{TiO}_2$  and hydrogen ion (Eq. 18).  $\text{TiO}_2$  becomes oxide film on the surface of the titanium as a barrier layer. Meantime,  $\text{TiO}_2$  is etched by  $\text{F}^-$  and many holes form in the film (Eq. 19). With the processing time increasing, the holes become deeper and form nanotubes. When the anodization rate of Ti is equal to the etching rate of  $\text{TiO}_2$ , the process reaches to a steady-state. The length of nanotubes keeps unchanged.

$\text{F}^-$  ion plays an important role in synthesizing  $\text{TiO}_2$  nanotubes. Fig. 10 shows the results of NTs obtained from different solutions with and without  $\text{F}^-$ . Without  $\text{F}^-$  the  $\text{TiO}_2$  is flat without porous structure. With  $\text{F}^-$ , reaction (Eq.19) occurs.  $\text{F}^-$  ion generates  $[\text{TiF}_6]^{2-}$  which is the driving force of etching  $\text{TiO}_2$ .  $\text{H}^+$  can enhance the etching ability of  $\text{F}^-$ .  $[\text{TiF}_6]^{2-}$  ions owing the small diameter can easily move through  $\text{TiO}_2$  crystal lattice. Comparing the electrolytes containing  $\text{Cl}^-$  and  $\text{Br}^-$  (Chen X et al., 2007),  $\text{TiO}_2$  nanotubes arrays fabricated in electrolytes containing  $\text{F}^-$  have better quality. Fluoride concentration can affect the electrochemical characteristics (Beranek R et al., 2003). If the fluoride concentration is low (less than 0.05 wt. %), there are almost no fluoride ions. If the fluoride concentration is high (1 wt. %), no oxide formation can be observed.  $\text{Ti}^{4+}$  reacts with  $\text{F}^-$  immediately to form  $[\text{TiF}_6]^{2-}$ . The maximum nanotube length is about 500 nm synthesized in HF electrolytes. The maximum length is several micron meters using NaF and  $\text{NH}_4\text{F}$  electrolytes.

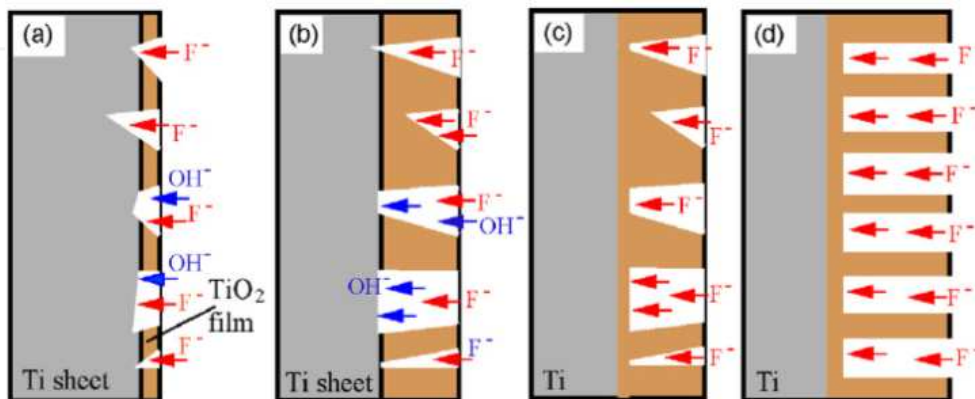


**Figure 11.** Self-organization of  $\text{TiO}_2$  nanotubes in  $\text{F}^-$  containing solutions. (Gan Y et al., 2011).

The mechanism of  $\text{TiO}_2$  growth can be shown in Fig. 11.  $\text{TiO}_2$  grows on the Ti substrate gradually. With the  $\text{TiO}_2$  film being thicker and thicker,  $\text{TiO}_2$  has the function of a protecting film to slow down the Ti dissolution. With the development of  $\text{F}^-$  etching  $\text{TiO}_2$ , the self-organized  $\text{TiO}_2$  nanotubes form as illustrated in Fig.11d.

### 7.2.2. Synthesis of $\text{TiO}_2$ nanotubes using organic electrolytes

Organic electrolytes containing  $\text{F}^-$  have some advantages. In 2005, Ruan CM et al. used dimethyl sulfoxide (DMSO) and ethylalcohol (1:1) as electrolytes for fabricating  $\text{TiO}_2$  nanotubes with a length of 2.3  $\mu\text{m}$ . Macak MJ et al., (2005) used glycerin synthesized  $\text{TiO}_2$  nanotubes with 7  $\mu\text{m}$  length. The maximum length could over 1000  $\mu\text{m}$ . Prakasam HE et al., (2007), using ethylene glycol with 1%-3%  $\text{H}_2\text{O}$  volume and 0.1% to 0.5 % wt of  $\text{NH}_4\text{F}$  solution, anodized Ti foil for 17 h at 20, 40, 50, 60 and 65 V. The result showed that with the increase in the voltage, the inner diameter, outer diameter and length of nanotubes were increased. The maximum values are 135 nm, 185 nm and 105  $\mu\text{m}$ , respectively. The nanotubes grow rate is 15  $\mu\text{m}/\text{h}$ . The important factor to affect the length of the nanotubes is the water content. The water volume content should be under 5% for obtain good quality of nanotubes. The morphology of  $\text{TiO}_2$  nanotubes formed in organic electrolysis more smooth and orderly. Besides, the nanotubes have higher photocatalytic efficiencies.

Non- $\text{F}^-$  electrolytes were also used (Allam N et al., 2007) for the environmental protection purpose. Pulse anodization (Chanmanee W et al., 2008) generated  $\text{TiO}_2$  nanotubes with good photoelectrochemical property. Glancing angle deposition (GLAD) was used to obtain Ti films. The anodization of the Ti films produced nanotubes and nanorods (NRs) on a glass substrate. Even brush type nanostructures (BTNs) were obtained (Pihosh Y et al., 2009) as shown in Fig. 12. As compared with the plate counterparts, the  $\text{TiO}_2$  NRs, NTs and BTNs have significantly higher photocatalytic activity under Vis-light and UV illumination. The NTs and BTNs have better photocatalytic activity than the NRs because of their larger surface areas. The BTNs can be obtained by andoization of NRs in base.

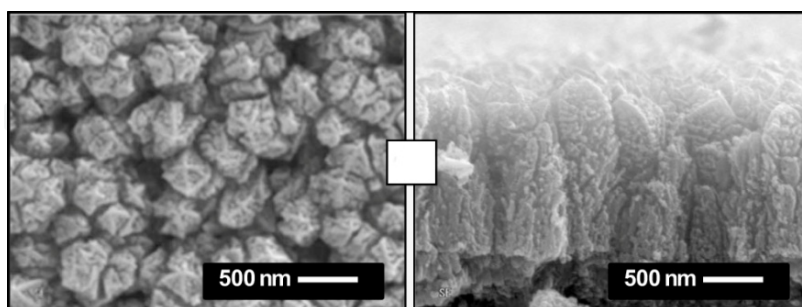


**Figure 12.** SEM images of brush type nanostructures (BTNs). (Pihosh Y et al., 2009).

## 7.3. Post-treatment of $\text{TiO}_2$ nanostructures

### 7.3.1. Annealing

The purpose of annealing is to change the morphology of  $\text{TiO}_2$  nanotubes from amorphous to crystalline (anatase or rutile). Over the past 10 to 15 years, there were a large number of

researchers focusing on annealing. Stem N et al., (2011), thermal treated TiO<sub>2</sub> at 1000 °C in wet N<sub>2</sub> for 2 hours, which enhances the photocatalytic performance. Wang MC et al., (2012), showed that annealing temperature affected photocatalytic capability of N-doped TiO<sub>2</sub> thin films. The temperature ranges from 250 °C to 550 °C. The time lasts for 1 hour. Below 350 °C, the surface roughness is low. The photocatalytic activity is the highest after the 350 °C annealing. Lin JY et al., (2011), applied the rapid thermal annealing (RTA) method. The temperatures been used that were 700, 800, 900, 1000 and 1100 °C. The temperate increasing rate was 5 °C/s. The total annealing time was 30 s in oxygen. Through the X-ray diffraction (XRD) examination, it was found that oxygen-related defects were reduced when the TiO<sub>2</sub> nanotubes changed from amorphous to anatase phase. Fang D et al., (2011), studied high temperate calcinations. TiO<sub>2</sub> nanotubes were exposed at the temperatures of 450, 600, 800, and 900°C. The results (Fig. 13) show that 450 °C helps generate a pure anatase phase. At 600 °C, a mixed phase of anatase and rutile can be got. At 800 °C, pure anatase phase grows into large crystallites. As the conclusion, 450 °C is the best calcination temperature. Bauer S et al., (2011), showed that the nanotube's size affects the crystal phase. When the nanotube's diameter is smaller than 30 nm, it is more likely to form rutile. In contrary, when the diameter is larger than 30 nm, anatase can be obtained. Not only the temperate, the type of gases used also affects the properties of the nanotubes (Sang LX et al., 2011). Annealing in air (TNT-A), nitrogen (TNT-N) and 5% hydrogen/nitrogen (TNT-H) generate the similar morphology and band gap. But the difference in the UV absorption photocurrent density exists. The maximum photocurrent density is 0.60 mA/cm<sup>2</sup> for the nanotubes named as TNT-H. The minimum is 0.27 mA/cm<sup>2</sup> for TNT-A. TNT-H has more surface defects. The more surface defects, the higher the photocurrent was generated.

On the contrary to traditional annealing process, Liu JM et al., (2011), performed vacuum annealing and multi-cycle annealing on the Nb-doped TiO<sub>2</sub> thin film. During the three-cycle vacuum annealing, the TiO<sub>2</sub> was heated up to 550 °C (0.05 Pa air pressure) for 1 hour in one cycle. This process was repeated for three times. In another experiment, the TiO<sub>2</sub> film was held at 550 °C at 5 Pa air pressure for 1 hour. Then the annealing was repeated for three times. These two different procedures both can improve the conductivity of the Nb-doped TiO<sub>2</sub> thin film. At different annealing temperatures, the TiO<sub>2</sub> nanotubes showed different photoelectrochemical characteristics (Tang Y et al., 2008). The treatment temperatures are in the range from 300 °C to 550 °C. Again, the sample annealed at 450 °C showed better performance under UV light. With the UV on, the nanotube electrode showed good photoelectric current stability. When the UV was off, the photocurrent quickly decreased to the initial value.

### 7.3.2. Ultrasonic clean

During anodization synthesis, TiO<sub>2</sub> nanotubes formed, but unexpected deposits may also be on the nanotubes. They can be cleaned by ultrasonic waves (Cai QY et al., 2005). Xu H et al., (2011), applied ultrasonic waves to clean the surface of TiO<sub>2</sub> nanotubes for different time periods. They employed the ultrasonic wave with the power of 80 W at 40 kHz. 9 min is the best treatment time for cleaning the nanotubes. When the time was extended to 40 min, the nanotubes were broken. The nanotubes were peeled off from the Ti completely at 60 min.

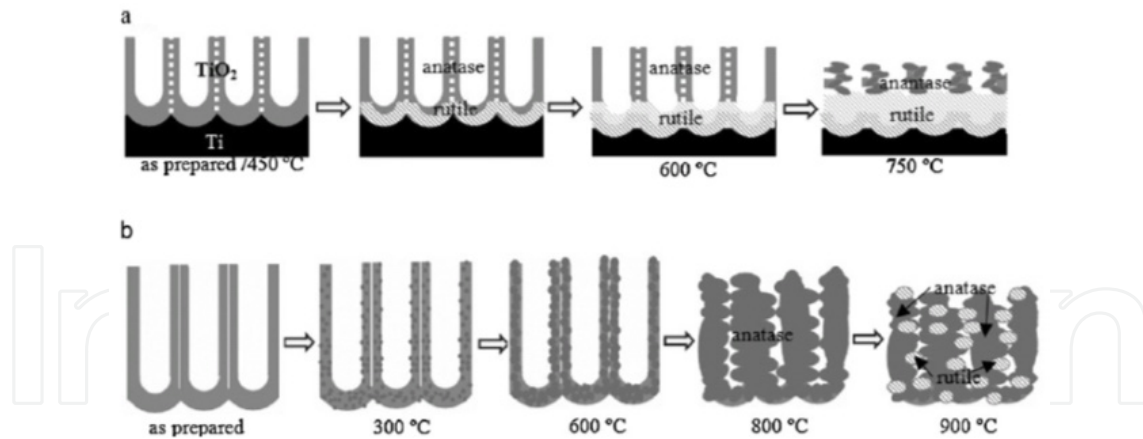


**Figure 13.** Annealing treatment of TiO<sub>2</sub> nanotubes (a) with Ti substrate, (b) free standing nanotubes. (Fang D et al., 2011).

### 7.3.3. Doping

There are two main limitations of pure TiO<sub>2</sub> nanotubes

1. Pure TiO<sub>2</sub> can only absorb UV light of wavelength shorter than 400 nm because the band gap of TiO<sub>2</sub> is 3.2 eV, which means that pure TiO<sub>2</sub> can only utilize 6% solar energy. The visible light has the energy band gaps from 1.8 eV to 3.1 eV.
2. High electrical resistance of pure TiO<sub>2</sub> at the room temperature results in very low electron transfer rate. This causes electric energy loss. The converted heat energy dissipates into ambient. At 20 °C, TiO<sub>2</sub> is not a conductor. Only when the temperature rises to 400 °C, the resistance of TiO<sub>2</sub> becomes lower.

Direct doping is one way to overcome the limitations of pure titania. Another method of doping is to stack different materials which have different band gaps. That could make hybrid photoanode (HPE) as first reported by Morisaki H et al., (1976).

Some noble metals doped to TNTs such as gold (Malwadkar SS et al., 2009), silver (Guo GM et al., 2009), platinum can improve the photocatalytic activity of the TNTs. This is because these noble metals can inhibit recombination of electron (Chan SC et al., 2005). Metal doped-TNTs for photo fuel cell applications are reported.

In addition to using noble metals, Macak JM et al., (2007) showed doping copper by electrodeposition. First, synthesis of TiO<sub>2</sub> nanotubes which have low conductivity especially at the bottom of the nanotubes was carried out. Second, using an aqueous electrolyte, about 1% of Ti<sup>4+</sup> in the TiO<sub>2</sub> outer layer was converted into Ti<sup>3+</sup> (Ti<sup>4+</sup> + e<sup>-</sup> + H<sup>+</sup> = Ti<sup>3+</sup>H<sup>+</sup> and 2H<sup>+</sup> + 2e<sup>-</sup> = H<sub>2</sub>). With Ti<sup>3+</sup>, the mobility gap of TiO<sub>2</sub> was reduced from 3.2 eV to 2.4 eV and the bottom of the nanotubes become highly conductive. The third step is to dope the nanotubes with Cu. Since the bottom has a high conductivity with Ti<sup>3+</sup> and H<sup>+</sup>, Cu is easily be doped in the nanotubes by a current pulsing electroplating approach.

Sun L et al., (2009), fabricated Fe-doped TNTs using Fe ion containing electrolytes. This study shows that the content of Fe<sup>3+</sup> is a significant factor affecting the photo catalysis

capacity. They used three  $\text{Fe}(\text{NO}_3)_3$  solutions for comparison. The concentrations are 0.05 M, 0.1 M and 0.2 M. The result shows that 0.1 M  $\text{Fe}(\text{NO}_3)_3$  doped TNTs have the maximum photo current and photocatalytic degradation rate. 0.15 M  $\text{Fe}(\text{NO}_3)_3$  doped nanotubes have the maximum absorbance under UV-Vis. Different application need different  $\text{Fe}(\text{NO}_3)_3$  contents. Tu YF et al., (2010), employed template-based LPD method to dope Fe to TNTs. Redshift of the absorption was found. The best Fe content was 5.9 at %. The doped-TNTs achieved the best efficiency of photo catalysis under visible light. Wu Q et al., (2012), fabricated Fe-doped ( $\text{Fe}_2\text{O}_3$  and  $\text{Fe}^{3+}$ ) with ultrasound assisted impregnating calcinations method. Results showed that  $\text{Fe}_2\text{O}_3$  went into the TNTs and  $\text{Fe}^{3+}$  into the  $\text{TiO}_2$  lattice. The operation time and temperatures affect the photo responses of Fe-doped TNTs. Ultrasound treating for 5 min following by annealing at 500 °C provides NTNs the highest photo catalysis efficiency.

C and N doping are non-metal doping examples. B, P, and other nonmetallic dopants are also used. Nitrogen is the earliest, most effective and most studied doping element for TNTs. There are many methods to dope nitrogen into TNTs such as annealing TNTs in ammonia (Vitiello RP, et al., 2006), ion implantation (Ghicov A et al., 2006) etc. Asahi R et al., (2001), doped  $\text{TiO}_2$  with nitrogen using a solution method. Vitiello RP et al., (2006), showed a simple method for making N-doped TNTs, which is treating TNTs at 300-600 °C in  $\text{NH}_3$  atmosphere. Results showed that 500 °C- 600 °C is the best annealing temperate range at which TNTs transfer to anatase and have the most effective photoresponse. Xu JJ et al., (2010), showed difference in photo catalytic activity between N-doped and Non-doped  $\text{TiO}_2$  nanotubes under Vis-light. The photocurrent density of N-doped nanotubes was twice as that of the non-doped nanotubes under visible light illumination. Yuan J et al., (2006), synthesized N-doped  $\text{TiO}_2$  by heating urea with  $\text{TiO}_2$  at 300-700 °C. The doped  $\text{TiO}_2$  can absorb light with the wavelength up to 600 nm. The result shows that urea changes to chemisorbed  $\text{N}_2$  and substituted N staying in the  $\text{TiO}_2$ .

Liu ZY et al., (2009), doped carbon into TNTs for solar photochemical cell hydrogen generation. Shaban YA et al., (2007), studied the fabrication time and temperature effects on grooved and non-grooved Ti metal sheet doped with carbon for photochemical catalysis. The result shows that the grooved sample has higher photocurrent density than the non-grooved one. The grooved simple with a depth of 0.005 inch has the maximum photo conversion efficiency of 11.37 % (treated at 820 °C, 18 minutes, thermal flame oxidation, tested in 5.0 M KOH, illuminated by a 150 W Xenon lamp). The non-grooved simple, 0.003 inch grooved one, and 0.001 inch groove done have the maximum photo conversion efficiency of 9.08 %, 8.68 %, 7.20 %, respectively under the same treatment condition.

Co-doping multiple elements was also applied to  $\text{TiO}_2$  nanotubes. Tungsten and nitrogen co-doping is a typical example (Shen YF et al., 2008). Nitrogen and sulfur (Yan GT et al., 2011), fluorine and boron (Su YL et al., 2008), Pt and N (Huang LH et al., 2007) co-doping has also been studied. Liu SH et al., (2009), developed a carbon and nitrogen co-doping method by adding 5 mg polyvinyl alcohol (PVA) and 20 mg urea. Then calcination was performed in nitrogen at 600 °C. The photocurrent density is 3 times, 2 times, and 1.2 times

compared with the non-doped, C-doped and N-doped TiO<sub>2</sub> nanotubes under solar light and 0.2 V bias-potential combined excitation. He HC et al., (2011), doped Pt-Ni into NTNs using pulsed electrodeposition method. The photo catalytic activity is better than that of only Pt-doped NTNs. Pt-Ni doped NTN is a good anode material for photo fuel cell (direct methanol type). The performance of co-doped TNT is better than that of Pt doped one. Huang LH et al., (2007), synthesized Pt-N doped TNTs by two steps. First, they obtained N-doped TNTs. Second, they used H<sub>2</sub>PtCl<sub>6</sub> solution to supply Pt, resulting in Pt-N co-doping. N-doping can enhance the photo response activity and Pt-doping can strengthen the electron separation from holes. Ag can be deposited into N-doped TNTs (Zhang SS et al., 2011), via electrochemical deposition in a 0.2 g/L AgNO<sub>3</sub> solution. The result shows that the average photocurrent density of the Ag/N-doped TiO<sub>2</sub> nanotubes is 6 times higher.

Li XQ et al., (2011), developed the CdS nanoparticle and CuTsPc molecule co-doped TNTs. The I-V curve shows that CdS-CuTsPc has the maximum photocurrent density as compared with CdS-CuTsPc, CdS-CuPc, CdS, and CuTsPc doped TNTs. Jia FZ et al., (2012), successfully processed ZnS-In<sub>2</sub>S<sub>3</sub>-Ag<sub>2</sub>S doped TiO<sub>2-x</sub>S<sub>x</sub> by a two-step (anodization and solvothermal) approach. Zhang X et al. (2009), doped PW<sub>12</sub>O<sub>40</sub><sup>3-</sup> and Cr<sup>3+</sup> into TNTs through the anodization and impregnation methods. The function of Cr<sup>3+</sup> is narrowing the band gap of TiO<sub>2</sub>. They have found that the synergetic factor is 1.42. Su Y et al., (2008), doped nitrogen and fluorine into TNTs. They simply used anodization (20 V) of Ti in the C<sub>2</sub>H<sub>2</sub>O<sub>4</sub>·2H<sub>2</sub>O+NH<sub>4</sub>F electrolyte through TiO<sub>2</sub> self-organization. After annealing at 400°C, N-F-doped TNTs showed very good photocatalytic ability and stability. The efficiency of methyl orange (MO) decomposition test is higher than 97%. This method avoids using ammonia which is hazardous. With CeO<sub>2</sub> nanoparticles being doped into TNTs, enhanced charge storage capacity of TNTs was achieved (Wen H et al., 2011). Wang J et al., (2012), reported a C<sub>3</sub>N<sub>4</sub> doped TiO<sub>2</sub> nanorod. The UV-Vis absorbance ability of this modified material is as twice as that of the TiO<sub>2</sub>.

## 8. Conclusions

Photoelectrochemical fuel cells have experienced fast development recently because of the progress in nanomaterials. Using various materials processing techniques, it is possible to obtain various nanostructure forms such as nanoparticles, nanorods, nanothin film and nanotubes for photo fuel cell applications. There are many ways for fabricating nanostructures including hydro/solvothermal method, template-assisted method, sol-gel method, microwave irradiation method and electrochemical direct anodization method. Electrochemical anodization becomes a popular method in recent years because it is easy to control the size of nanotubes. Typical photo sensitive materials such as TiO<sub>2</sub>, WO<sub>3</sub>, Fe<sub>2</sub>O<sub>3</sub>, CuO and ZnO have been studied. These materials have different band gaps and many researchers reported how to enhance the photo response of them. Doping is a significant and efficient method for improving the photo response of nanomaterials. Metal doping and Non-metal doping are two major types. Besides, organic doping, co-doping alloys and multi-component materials also result in good performance of PEFCs. In summary, PEFCs

represent promising energy conversion systems. Future studies should focus on increasing the photoelectric energy conversion efficiency.

## Author details

Kai Ren and Yong X. Gan

*Department of Mechanical, Industrial and Manufacturing Engineering, College of Engineering, University of Toledo, Toledo, OH, USA*

## 9. References

- Allam N, Grimes C. Formation of vertically oriented TiO<sub>2</sub> nanotube arrays using a fluoride free HCl aqueous electrolyte . *Journal of Physical Chemistry C*. 2007;111; 13028-13032.
- Antoniadou M, Kondarides D , Labou D, Neophytides S , Lianos P. An efficient photoelectrochemical cell functioning in the presence of organic wastes. *Solar Energy Materials & Solar Cells*. 2010; 94; 592–597.
- Antoniadou M, Lianos P. Photoelectrochemical oxidation of organic substances over nanocrystalline titania: Optimization of the photoelectrochemical cell. *Catalysis Today*. 2009; 144; 166-171.
- Antoniadou M, Lianos P. Production of electricity by photoelectrochemical oxidation of ethanol in a PhotoFuelCell. *Applied Catalysis B: Environmental*. 2010; 99; 307-313.
- Asahi R, Morikawa T, Ohwaki T, Aoki K, Taga Y. Visible-light photocatalysis in nitrogen-doped titanium oxides. *Science*. 2001; 293; 269-271.
- Bak T, Nowotny J, Rekas M, Sorrell CC. Photo-electrochemical hydrogen generation from water using solar energy. Materials-related aspects. *International Journal of Hydrogen Energy*. 2002;27:991–1022.
- Bauer S, Pittrof A, Tsuchiya H, Schmuki P. Size-effects in TiO<sub>2</sub> nanotubes: Diameter dependent anatase/rutile stabilization. *Electrochemistry Communications*. 2011; 13; 538–541.
- Beranek R, Hildebrand H, Schmuki P. Self-organized porous titanium oxide prepared in H<sub>2</sub>SO<sub>4</sub>/HF electrolytes. *Electrochemical and Solid-State Letters*. 2003; 6; B12-B14.
- Cai QY, Paulose M, Varghese OK, Grimes CA. The effect of electrolyte composition on the fabrication of self-organized titanium oxide nanotube arrays by anodic oxidation. *Journal of Materials Research*. 2005 ,20 : 230 -236.
- Chakrapani V, Thangala J, Sunkara MK. WO<sub>3</sub> and W<sub>2</sub>N nanowire arrays for photoelectrochemical hydrogen production. *International Journal of Hydrogen Energy*. 2009; 34; 9050-9059.
- Chan SC, Barteau MA. Preparation of highly uniform Ag/TiO<sub>2</sub> and Au/TiO<sub>2</sub> supported nanoparticle catalysts by photodeposition. *Langmuir*. 2005; 21; 5588-5595.
- Chang C, Wang C, Tseng C, Cheng K, Hourng L, Tsai B. Self-oriented iron oxide nanorod array thin film for photoelectrochemical hydrogen production. *International Journal of Hydrogen Energy*. 2012. Article in press.

- Chanmanee W, Watcharenwong A, Chenthamarakshan C R, Kajitvichyanukul P, Tacconi N, and Rajeshwar K. Formation and characterization of self-organized TiO<sub>2</sub> nanotube arrays by pulse anodization. *Journal of the American Chemical Society*. 2008; 130; 965-974.
- Chen X, Schriver M, Suen T, Mao SS. Fabrication of 10 nm diameter TiO<sub>2</sub> nanotube arrays by titanium anodization. *Thin Solid Films*. 2007; 515 ;8511 -8514.
- Chen XB, Mao SS. Titanium dioxide nanomaterials: synthesis, properties, modifications and applications. *Chemical Reviews*. 2007; 107; 2891-2959.
- Chiang C, Aroh K, Franson N, Satsangi V, Dass S, Ehrman S. Copper oxide nanoparticle made by flame spray pyrolysis for photoelectrochemical water splitting -Part II. Photoelectrochemical study. *International Journal of Hydrogen Energy*. 2011;36;15519-15529.
- Fang D, Luo ZP, Huang KL, Lagoudas DC. Effect of heat treatment on morphology, crystalline structure and photocatalysis properties of TiO<sub>2</sub> nanotubes on Ti substrate and freestanding membrane. *Applied Surface Science*. 2011; 257; 6451-6461.
- Fen LB, Han TK, Nee NM, Ang BC, Johan MR. Physico-chemical properties of titania nanotubes synthesized via hydrothermal and annealing treatment. *Applied Surface Science*. 2011; 258;431- 435.
- Fujishima A, Honda K. Electrochemical photolysis of water at a semiconductor electrode. *Nature*. 1972; 238: 37-38.
- Gan Y, Gan B, Su L. Biophotofuel cell anode containing self-organized titanium dioxide nanotube array. *Materials Science and Engineering B*. 2011; 176; 1197– 1206.
- Ghicov A, Aldabergerova S, Tsuchiya H, Schmuki P. TiO<sub>2</sub>-Nb<sub>2</sub>O<sub>5</sub> nanotubes with electrochemically tunable morphologies. *Angewandte Chemie International Edition*. 2006; 45; 6993-6996.
- Ghicov A, Macak JM, Tsuchiya H, Kunze J, Haeublein V, Frey L, Schmuki P. Ion implantation and annealing for an efficient N-doping of TiO<sub>2</sub> nanotubes. *Nano Letters*. 2006;6;1080–1082.
- Gratzel M. Photoelectrochemical cells. *Nature*. 2001; 414; 338-344.
- Guo GM, Yu BB, Yu P, Chen X. Synthesis and photocatalytic applications of Ag/TiO<sub>2</sub>-nanotubes. *Talanta*. 2009;79; 570–575.
- He HC, Xiao P, Zhou M, Zhang YH, Jia YC, Yu SJ. Preparation of well-distributed Pt-Ni nanoparticles on/into TiO<sub>2</sub> NTs by pulse electrodeposition for methanol photoelectro-oxidation. *Catalysis Communications*. 2011; 16; 140–143.
- Huang LH, Sun C, Liu YL. Pt/N-codoped TiO<sub>2</sub> nanotubes and its photocatalytic activity under visible light. *Applied Surface Science*. 2007; 253; 7029–7035.
- Isimjan TT, Rohani S, Ray AK. Photoelectrochemical water splitting for hydrogen generation on highly ordered TiO<sub>2</sub> nanotubes fabricated by using Ti as cathode. *International Journal of Hydrogen Energy*. 2012;37;103-106.
- Jia FZ, Yao ZP, Jiang ZH, Li CX. Preparation of carbon coated TiO<sub>2</sub> nanotubes film and its catalytic application for H<sub>2</sub> generation. *Catalysis Communications*. 2011; 12; 497–501.
- Kaneko M, Nemoto J, Ueno H, Gokan N, Ohnuki K, Horikawa M, Saito R, Shibata T. Photoelectrochemical reaction of biomass and bio-related compounds with nanoporous

- TiO<sub>2</sub> film photoanode and O<sub>2</sub> reducing cathode. *Electrochemistry Communications*. 2006; 8; 336-340.
- Kasuga T, Hiramatsu M, Hoson A, Sekino T, Niihara K. Formation of titanium oxide nanotube, *Langmuir*. 1998; 14; 3160–3163.
- Lan Y, Gao XP, Zhu HY, Zheng ZF, Yan TF, Wu F, Ringer SP, Song DY. Titanate nanotubes and nanorods prepared from rutile powder. *Advanced Functional Materials*. 2005;15; 1310-1318.
- Li XQ, Cheng Y, Liu LF, Mu J. Enhanced photoelectrochemical properties of TiO<sub>2</sub> nanotubes co-sensitized with US nanoparticles and tetrasulfonated copper phthalocyanine. *Colloids and Surfaces A: Physicochemical and Engineering Aspects*. 2011;353; 226–231.
- Lianos P. Production of electricity and hydrogen by photocatalytic degradation of organic wastes in a photoelectrochemical cell. The concept of the Photofuelcell: A review of a re-emerging research field. *Journal of Hazardous Materials*. 2010; 185; 575-590.
- Lin JY, Chou YT, Shen JL, Yang MD, Wu CH, Chi GC, Chou WC, Ko CH. Effects of rapid thermal annealing on the structural properties of TiO<sub>2</sub> nanotubes. *Applied Surface Science*. 2011; 258; 530- 534.
- Liu H, Tao L, Shen WZ. Optimal self-organized growth of small anodic TiO<sub>2</sub> nanotubes with "micro-annealing" effect under complex conditions via reaction-diffusion approach. *Electrochimica Acta*. 2011; 56 ; 3905-3913.
- Liu JM, Zhao X, Duan L, Cao M, Sun H, Shao J, Chen S, Xie H, Chang X, Chen C. Influence of annealing process on conductive properties of Nb-doped TiO<sub>2</sub> polycrystalline films prepared by sol-gel method. *Applied Surface Science*. 2011; 257;10156– 10160.
- Liu S, Yang L, Xu S, Luo S, Cai Q. Photocatalytic activities of C–N-doped TiO<sub>2</sub> nanotube array/carbon nanorod composite. *Electrochemistry Communications*. 2009; 11;1748–1751.
- Liu SH, Yang LX, Xu SH , Luo SL, Cai QY. Photocatalytic activities of C–N-doped TiO<sub>2</sub> nanotube array/carbon nanorod composite. *Electrochemistry Communications*. 2009;11;1748-1751.
- Liu Y, Li J, Zhou B, Li X, Chen H, Chen Q, Wang Z, Li L, Wang J, Cai W. Efficient electricity production and simultaneously wastewater treatment via a high-performance photocatalytic fuel cell. *Water research*. 2011; 45; 3991-3998.
- Liu ZY, Pesic B, Raja KS, Rangaraju RR, Misra M. Hydrogen generation under sunlight by self ordered TiO<sub>2</sub> nanotube arrays. *International Journal of Hydrogen Energy*. 2009; 34; 3250 -3257.
- Macak J M, Tsuchiya H, Ghicov A, Yasuda K, Hahn R, Bauer S, Schmuki P. TiO<sub>2</sub> nanotubes: Self-organized electrochemical formation, properties and applications. *Current Opinion in Solid State and Materials Science*. 2007; 1; 3–18.
- Macak J M, Tsuchiya H., P Schmuki. High-aspect-ratio TiO<sub>2</sub> nanotubes by anodization of titanium. *Angewandte Chemie International Edition*. 2005; 44 ;2100 -2102.
- Macak J M, Tsuchiya H., Taveira L, Aldabergerova S, Schmuki P. Smooth anodic TiO<sub>2</sub> nanotubes. *Angewandte Chemie International Edition*. 2005; 44 : 7463-7465.
- Macak JM, Gong BG, Hueppe M, Schumk P, Filling of TiO<sub>2</sub> Nanotubes by self-Doping and Electrodeposition. *Advanced Materials*. 2007;19;3027-3031.

- Mahajan V, Mohapatra S, Misra M. Stability of TiO<sub>2</sub> nanotube arrays in photoelectrochemical studies. *International Journal of Hydrogen Energy*. 2008; 33; 5369-5374.
- Malwadkar SS, Gholap RS, Awate SV, Korake PV, Chaskar MG, Gupta NM. Physico-chemical, photo-catalytic and O<sub>2</sub>-adsorption properties of TiO<sub>2</sub> nanotubes coated with gold nanoparticles. *Journal of Photochemistry and Photobiology A: Chemistry*. 2009; 203; 24-31.
- Miller EL, Rocheleau RE, Deng XM. Design considerations for a hybrid amorphous silicon/photoelectrochemical multijunction cell for hydrogen production. *International Journal of Hydrogen Energy*. 2003; 28; 615-623.
- Minggu LJ, Daud WRW, Kassim MB, Cronin SB. An overview of photocells and photoreactors for photoelectrochemical water splitting. *International Journal of Hydrogen Energy*. 2010;35;5233-5244.
- Morisaki H, Watanabe T, Iwase M, Yazawa K. Photoelectrolysis of water with TiO<sub>2</sub> covered solar-cell electrodes. *Appl Phys Lett*. 1976; 29; 338-340.
- Ollis DF. Photocatalytic purification and remediation of contaminated air and water. *Comptes Rendus Del Academie Des Sciences Serie II Fascicule C-Chimie*. 2000; 3; 405-411.
- Park KW, Han SB, Lee JM. Photo(UV)-enhanced performance of Pt-TiO<sub>2</sub> nanostructure electrode for methanol oxidation. *Electrochemistry Communications*. 2007; 9; 1578-1581.
- Patsoura A., Kondarides DI, Verykios XE. Enhancement of photoinduced hydrogen production from irradiated Pt/TiO<sub>2</sub> suspensions with simultaneous degradation of azo-dyes. *Applied Catalysis B: Environmental*. 2006; 64 ;171-179.
- Pihosh Y, Turkevych I, Ye J, Goto M, Kasahara A, Kondo M, Tosa M. Photocatalytic Properties of TiO<sub>2</sub> Nanostructures Fabricated by Means of Glancing Angle Deposition and Anodization. *Journal of the Electrochemical Society*. 2009;156;160-165.
- Prakasam HE, Shankar K, Paulose M, Varghese OK, Grimes, CA. A new benchmark for TiO<sub>2</sub> nanotube array growth by anodization. *Journal of Physical Chemistry C*. 2007; 111; 7235-7241.
- Reber JF, Meier K. Photochemical production of hydrogen with zinc-sulfide suspensions. *Journal of Physical Chemistry*. 1984; 88; 5903-5913.
- Ruan CM, Paulose M, Varghese OK, Mor GK, Grimes CA. Fabrication of highly ordered TiO<sub>2</sub> nanotube arrays using an organic electrolyte. *Journal of Physical Chemistry B*. 2005; 109; 15754-15759.
- Sakthivel S, Shankar MV, Palanichamy M, Arabindoo B, Bahnemann DW, Murugesan V. Enhancement of photocatalytic activity by metal deposition: characterisation and photonic efficiency of Pt, Au and Pd deposited on TiO<sub>2</sub> catalyst. *Water Research*. 2004; 38; 3001-3008.
- Sang LX, Zhang ZY, Ma CF. Photoelectrical and charge transfer properties of hydrogen-evolving TiO<sub>2</sub> nanotube arrays electrodes annealed in different gases. *International Journal of Hydrogen Energy*. 2011; 36; 4732-4738.

- Seo HK, Kim GS, Ansari SG, Kim YS, Shin HS, Shim KH, Suh EK. A study on the structure/phase transformation of titanate nanotubes synthesized at various hydrothermal temperatures. *Solar Energy Materials and Solar Cells*. 2008; 92; 1533–1539.
- Shaban YA, Khan SUM. Surface grooved visible light active carbon modified (CM)-n-TiO<sub>2</sub> thin films for efficient photoelectrochemical splitting of water. *Chemical Physics*. 2007; 339; 73-85.
- Shankar K, Mor GK, Prakasam HE, Yoriya S, Paulose M, Varghese OK, Grimes CA. Highly-ordered TiO<sub>2</sub> nanotube arrays up to 220 μm in length: use in water photoelectrolysis and dye-sensitized solarcells. *Nanotechnology*. 2007; 18; 065707.
- Shen YF, Xiong TY, Li TF, Yang K. Tungsten and nitrogen co-doped TiO<sub>2</sub> nano-powders with strong visible light response. *Applied Catalysis B: Environmental*. 2008; 83; 177-185.
- Sreekantan S, Wei LC. Study on the formation and photocatalytic activity of titanate nanotubes synthesized via hydrothermal method. *Journal of Alloys and Compounds*. 2010; 490 ; 436–442.
- Stem N, Chinaglia EF, dos Santos Filho SG. Microscale meshes of Ti<sub>3</sub>O<sub>5</sub> nano- and microfibers prepared via annealing of C-doped TiO<sub>2</sub> thin films. *Materials Science and Engineering B*. 2011; 176; 1190-1196.
- Su Y, Chen SO, Quan X, Zhao HM, Zhang YB. A silicon-doped TiO<sub>2</sub> nanotube arrays electrode with enhanced photoelectrocatalytic activity. *Applied Surface Science*. 2008; 255; 2167-2172.
- Su YL, Han S, Zhang XW, Chen XQ, Lei LC. Preparation and visible-light-driven photoelectrocatalytic properties of boron-doped TiO<sub>2</sub> nanotubes. *Materials Chemistry and Physics*. 2008; 110; 239–246.
- Sun L, Li J, Wang CL, Li F, Chen HB, Lin CJ. An electrochemical strategy of doping Fe<sup>3+</sup> into TiO<sub>2</sub> nanotube array films for enhancement in photocatalytic activity. *Solar Energy Materials and Solar Cells*. 2009; 93; 1875-1880.
- Tang Y, Tao J, Zhang Y, Wu T, Tao H, Bao Z. Preparation and Characterization of TiO<sub>2</sub> Nanotube Arrays via Anodization of Titanium Films Deposited on FTO Conducting Glass at Room Temperature. *ACTA Physico-Chimica Sinica*. 2008; 24; 2191-2197.
- Tu YF, Huang SY, Sang JP, Zou XW. Preparation of Fe-doped TiO<sub>2</sub> nanotube arrays and their photocatalytic activities under visible light. *Materials Research Bulletin*. 2010; 45; 224-229.
- Varghese OK, Gong DW, Paulose M, Grimes CA, Dickey EC. Crystallization and high-temperature structural stability of titanium oxide nanotube arrays. *Journal of Materials Research*. 2003; 18; 156 -165.
- Vitiello RP, Macak JM, Ghicov A, Tsuchiya H, Dick LFP, Schmuki P. N-Doping of anodic TiO<sub>2</sub> nanotubes using heat treatment in ammonia *Electrochemistry Communications*. 2006; 8; 544–548.
- Wang J, Zhang W. Modification of TiO<sub>2</sub> nanorod arrays by graphite-like C<sub>3</sub>N<sub>4</sub> with high visible light photoelectrochemical activity. *Electrochimica Acta*. 2012; 71; 10-16.

- Wang MC, Lin HJ, Wang CH, Wu HC. Effects of annealing temperature on the photocatalytic activity of N-doped TiO<sub>2</sub> thin films. *Ceramics International*. 2012;38; 195-200.
- Wen H, Liu Z, Yang Q, Li Y, Jerry Yu J. Synthesis and electrochemical properties of CeO<sub>2</sub> nanoparticle modified TiO<sub>2</sub> nanotube arrays. *Electrochimica Acta*. 2011; 56; 2914–2918.
- Wu Q, Ouyang JJ, Xie KP, Sun L, Wang MY, Lin CJ. Ultrasound-assisted synthesis and visible-light-driven photocatalytic activity of Fe-incorporated TiO<sub>2</sub> nanotube array photocatalysts. *Journal of Hazardous Materials*. 2012; 199; 410-417.
- Xu H, Zhang Q, Zheng CL, Yan W, Chu W. Application of ultrasonic wave to clean the surface of the TiO<sub>2</sub> nanotubes prepared by the electrochemical anodization. *Applied Surface Science*. 2011; 257; 8478–8480.
- Xu JJ, Ao YH, Chen MD, Fu DG. Photoelectrochemical property and photocatalytic activity of N-doped TiO<sub>2</sub> nanotube arrays. *Applied Surface Science*. 2010; 256; 4397–4401.
- Xu YM, Fang XM, Xiong JA, Zhang ZG. Hydrothermal transformation of titanate nanotubes into single-crystalline TiO<sub>2</sub> nanomaterials with controlled phase composition and morphology. *Materials Research Bulletin*. 2010; 45; 799-804.
- Yan GT, Zhang M, Hou J, Yang JJ. Photoelectrochemical and photocatalytic properties of N plus S co-doped TiO<sub>2</sub> nanotube array films under visible light irradiation. *Materials Chemistry and Physics*. 2011; 129; 553-557.
- Yuan J, Chen MX, Shi JW, Shanguan WF. Preparations and photocatalytic hydrogen evolution of N-doped TiO<sub>2</sub> from urea and titanium tetrachloride. *International Journal of Hydrogen Energy*. 2006; 31; 1326-1331.
- Yuan ZY, Su BL. Titanium oxide nanotubes, nanofibers and nanowires. *Colloids and Surfaces A: Physicochemical and Engineering Aspects*. 2004; 241; 173-183.
- Zeng X, Gan Y, Clark E, Su L. Amphiphilic and photocatalytic behaviors of TiO<sub>2</sub> nanotube arrays on Ti prepared via electrochemical oxidation. *Electrochemistry Communications* 2009;11; 1748–1751.
- Zhang SS, Peng F, Wang HJ, Yu H, Zhang SQ, Yang J, Zhao HJ. Electrodeposition preparation of Ag loaded N-doped TiO<sub>2</sub> nanotube arrays with enhanced visible light photocatalytic performance. *Catalysis Communications*. 2011; 12; 689–693.
- Zhang X, Lei L, Zhang J, Chen Q, Bao J, Fang B. Preparation of PW<sub>12</sub>O<sub>40</sub><sup>3-</sup>/Cr–TiO<sub>2</sub> nanotubes photocatalysts with the high visible light activity. *Separation and Purification Technology*. 2009; 67; 50–57.
- Zhang XW, Lei LC, Zhang JL, Chen QX, Bao JG, Fang B. A novel CdS/S-TiO<sub>2</sub> nanotubes photocatalyst with high visible light activity. *Separation and Purification Technology*. 2009; 68; 433-433.
- Zhao Q, Li M, Chu JY, Jiang TS, Yin HB. Preparation, characterization of Au (or Pt)-loaded titania nanotubes and their photocatalytic activities for degradation of methyl orange. *Applied Surface Science*. 2009; 255; 3773-3778.
- Zwilling V, Darque-Ceretti E, Boutry-Forveille A, David D, Perrin MY, Aucouturier M. Structure and physicochemistry of anodic oxide films on titanium and TA6V alloy. *Surf Interface Anal*. 1999 ; 27; 629-637.